IOPscience

HOME | SEARCH | PACS & MSC | JOURNALS | ABOUT | CONTACT US

Effect of radiative cascades on intensities of dielectronic satellites to He_{α}

This article has been downloaded from IOPscience. Please scroll down to see the full text article.

2009 Phys. Scr. 79 035303

(http://iopscience.iop.org/1402-4896/79/3/035303)

The Table of Contents and more related content is available

Download details:
The article was downloaded by: fnevgeny
IP Address: 132.77.4.129
The article was downloaded on 04/03/2009 at 16:49

Please note that terms and conditions apply.

Phys. Scr. **79** (2009) 035303 (8pp) doi:10.1088/0031-8949/79/03/035303

Effect of radiative cascades on intensities of dielectronic satellites to He_α

V A Bernshtam[1], Yu Zarnitsky[1], Yu Ralchenko[1,3], L A Vainshtein[2], L Weingarten[1] and Y Maron[1]

[1] Faculty of Physics, Weizmann Institute of Science, Rehovot 76100, Israel
[2] PN Lebedev Physical Institute, Russian Academy of Sciences, Moscow 117924, Russia

E-mail: vladimir.bernshtam@weizmann.ac.il

Received 17 August 2008
Accepted for publication 11 December 2008
Published 3 March 2009
Online at stacks.iop.org/PhysScr/79/035303

Abstract
Radiative cascades into autoionizing states $1s2l2l'$ in Li-like ions are studied. The correction function that describes the effect of cascades on level populations is calculated using the $1/Z$-expansion method for the range of nuclear charges $Z = 10$–30. It is shown that for the q-satellite, which is often used in hot plasmas for diagnostic purposes, the contribution of radiative cascades may be three orders of magnitude larger than the direct dielectronic capture. Time-dependent collisional–radiative modeling is used to calculate satellite intensities and determine spectra modifications due to radiative cascades.

PACS numbers: 32.80.Hd, 32.30.Rj, 34.80.Kw

(Some figures in this article are in colour only in the electronic version.)

1. Introduction

Dielectronic satellites to resonance lines of H- and He-like ions are widely used for diagnostics of high-temperature plasmas (see, for example, [1–3]). Important parameters such as electron temperature and density can be reliably inferred from the corresponding line ratios. This technique requires accurate calculation of rates of atomic processes that populate doubly excited autoionizing states. While dielectronic capture (DC) and inner-shell excitation are the most significant mechanisms, it is well known that radiative cascades from high-n levels may also be important [4–6]. The contributions of cascades are especially significant for those levels with small DC probabilities that are primarily populated via electron-impact excitation.

The cascade processes have been previously discussed in several papers. For instance, the effect of radiative cascades on dielectronic satellite spectra in H-like ions was investigated in detail in [4]. Recently, cascades affecting the most intense dielectronic satellites to the He_α resonance line in Ar XVII were discussed in relation to diagnostics of tokamak plasmas [5]. It was shown that cascades have the strongest effect on satellites q and r in Gabriel's designations [7] (or for levels K232 and K234 in the designations accepted in program MZ [8, 9]), whereas for other satellites the cascade processes were found to be unimportant.

In this paper, we calculate the contribution of radiative cascades from all high-n states to the intensities of the $1s^2 2l$–$1s2l'2l''$ satellites to the resonance line in He-like ions for elements from neon ($Z = 10$) to zinc ($Z = 30$). The calculation is performed with the $1/Z$-expansion code MZ [8, 9] which is widely used in satellite studies. The calculated corrections to the intensity factor Q_d are then included in time-dependent collisional–radiative calculations that explicitly demonstrate the importance of radiative cascades for several satellite lines.

2. Calculation of the correction function

In low-density plasmas, the intensity $I_s(i, j)$ of a dielectronic satellite line that is formed as a result of electron transition from a doubly excited state i to a state j can be given by the following expression [5]:

$$I_s(i, j) = C_1 N_{He} N_e \frac{Q_d(i, j)}{T_e^{3/2}} \gamma\,(i, T_e)\ e^{-E_s/T_e}, \qquad (1)$$

where C_1 is a numerical constant, N_{He} is the density of the He-like ion ground state, N_e is the electron density, T_e is the

[3] Permanent address: National Institute of Standards and Technology, Gaithersburg, MD 20899-8422, USA.

 © 2009 The Royal Swedish Academy of Sciences Printed in the UK

electron temperature, $Q_d(i, j)$ is the intensity factor [10] and E_s is the excitation energy of a satellite level above the He-like ground state. The intensity factor is defined as

$$Q_d(i, j) = \frac{g_i A_a(i, j_0) A_r(i, j)}{A_a^i + A_r^i},$$

where $A_r(i, j)$ and $A_a(i, j_0)$ are the radiative and autoionization transition rates from level i into levels j and j_0 (the ground state), and A_r^i and A_a^i are corresponding total rates.

In equation (1) $\gamma(i, T_e)$ is the correction function to the satellite intensity due to the cascades [4] defined as

$$\gamma\,(i, T_e) = 1 + \frac{1}{g_i A_a^i} \sum_{k>i} Q_d(k, i) e^{(E_i - E_k)/T_e}, \qquad (2)$$

where g_i is the statistical weight of level i. The summation extends over all $n \geqslant 3$ levels. The radiative cascades between the $n = 2$ levels have very small transition probabilities and, therefore, are neglected in what follows. The correction function $\gamma(i, T_e)$ only depends on the upper state i and is thus related to all lines originating from that doubly excited state. Without cascades, the correction function is unity, so that $\gamma(i, T_e) - 1$ represents the contribution of cascades to the intensity of a satellite line.

In the present work, the correction function of equation (2) was calculated with the $1/Z$-expansion code MZ. A detailed description of this package and relevant methods can be found elsewhere [8, 9]. The MZ code, which is extensively used for the determination of atomic characteristics of autoionizing states in highly charged ions (see e.g. [10, 11]), can compute all atomic data required for the calculation of cascades, namely, energy levels, radiative transition probabilities and autoionization rates. We explicitly calculated the contribution of transitions from levels $1s2ln l'$ with $3 \leqslant n \leqslant 7$, whereas the contributions from the higher-n levels were determined using the well-known $1/n^3$ scaling [9, 12]:

$$\sum_{k>i}^{\infty} Q_d(k, i) = \sum_{n=3}^{7} Q_d(k, i) + \sum_{n=8}^{\infty} Q_d(k, i)$$
$$= \sum_{n=3}^{7} Q_d(k, i) + Q_d(7, i) \sum_{n=8}^{\infty} \frac{7^3}{n^3}. \qquad (3)$$

Here, $Q_d(7, \mathrm{i})$ is the intensity factor for cascades from all $n = 7$ levels into a given level i.

In the following, we use two notation systems for designation of autoionizing $1s2l2l'$ states and corresponding satellite transitions. The MZ code [8] assigns upper-case letters to different configurations according to the scheme $C = 2s2p(^1P)1s$; $E = 2s^2(^1S)1s$; $F = 2p^2(^1S)1s$; $F = 2p^2(^1D)1s$; $M = 2p^2(^3P)1s$; $K = 2s2p(^3P)1s$; $P = 1s^22p$ and $S = 1s^22s$. Then, the spin S, orbital L and total J angular momenta are introduced by the $2S+1$, $2L+1$ and $2J+1$ values. Thus, for instance, a 1s2s2p level with the total values $S = 1/2$, $L = 1$, $J = 3/2$ and ^{3}P term for the 2s2p would be denoted as K234. Gabriel [7] introduced a lower-case letter notation for the $1s2l^2$–$1s2l'2l''$ transitions, which is presented in table 1 along with the corresponding MZ notations.

Table 1. Satellite notations according to Gabriel [7] and MZ code [8].

Designation in Gabriel's schema	Transition in LS-coupling notation	Transition in MZ notation
a	$1s^22p\,^2P_{3/2}$–$1s2p^2\,^2P_{3/2}$	P234–M234
b	$1s^22p\,^2P_{1/2}$–$1s2p^2\,^2P_{3/2}$	P232–M234
c	$1s^22p\,^2P_{3/2}$–$1s2p^2\,^2P_{1/2}$	P234–M232
d	$1s^22p\,^2P_{1/2}$–$1s2p^2\,^2P_{1/2}$	P232–M232
e	$1s^22p\,^2P_{3/2}$–$1s2p^2\,^4P_{5/2}$	P234–M436
f	$1s^22p\,^2P_{3/2}$–$1s2p^2\,^4P_{3/2}$	P234–M434
g	$1s^22p\,^2P_{1/2}$–$1s2p^2\,^4P_{3/2}$	P232–M434
h	$1s^22p\,^2P_{3/2}$–$1s2p^2\,^4P_{1/2}$	P234–M432
i	$1s^22p\,^2P_{1/2}$–$1s2p^2\,^4P_{1/2}$	P232–M432
j	$1s^22p\,^2P_{3/2}$–$1s2p^2\,^2D_{5/2}$	P234–F256
k	$1s^22p\,^2P_{1/2}$–$1s2p^2\,^2D_{3/2}$	P232–F254
l	$1s^22p\,^2P_{3/2}$–$1s2p^2\,^2D_{3/2}$	P234–F254
m	$1s^22p\,^2P_{3/2}$–$1s2p^2\,^2S_{1/2}$	P234–F212
n	$1s^22p\,^2P_{1/2}$–$1s2p^2\,^2S_{1/2}$	P232–F212
o	$1s^22p\,^2P_{3/2}$–$1s2s^2\,^2S_{1/2}$	P234–E212
p	$1s^22p\,^2P_{1/2}$–$1s2s^2\,^2S_{1/2}$	P232–E212
q	$1s^22s\,^2S_{1/2}$–$1s2s(^3S)2p\,^2P_{3/2}$	S212–K234
r	$1s^22s\,^2S_{1/2}$–$1s2s(^1S)2p\,^2P_{1/2}$	S212–K232
s	$1s^22s\,^2S_{1/2}$–$1s2s(^1S)2p\,^2P_{3/2}$	S212–C234
t	$1s^22s\,^2S_{1/2}$–$1s2s(^3S)2p\,^2P_{1/2}$	S212–C232
u	$1s^22s\,^2S_{1/2}$–$1s2s(^3S)2p\,^4P_{3/2}$	S212–K434
v	$1s^22s\,^2S_{1/2}$–$1s2s(^3S)2p\,^4P_{1/2}$	S212–K432

3. Discussion

The correction functions $\gamma(i, T_e)$ for all $1s2l2l'$ states were calculated for nuclear charges $Z = 10$–30. The results are presented in the appendix for several elements and for temperatures in the range $T_e = (0.3\text{–}2) \times \mathrm{IP_{Li}}$, where $\mathrm{IP_{Li}}$ is the ionization potential of the corresponding Li-like ion. These temperatures define a range where dielectronic satellites are normally quite strong. Figures 1 and 2 show the values of $\gamma(i, T_e) - 1$, which is the deviation from the no-cascade case, as a function of Z at $T_e = 2 \times \mathrm{IP_{Li}}$ and $0.5 \times \mathrm{IP_{Li}}$, respectively. As seen in figures 1 and 2, the corrections for most of the strongest dielectronic satellites (e.g. j, k, a, s, t and r) are small, typically at the level of a few per cent, which agrees with the similar calculations for Ar [5]. This is an anticipated result since the high direct DC rate (that corresponds to the inverse strong autoionization probability) dominates the population influx for the upper states of the corresponding levels. However, the weak satellites, such as v, u or h, are strongly affected by radiative cascades. For low-Z elements the correction function is on the order of 100 or even more, as shown in figures 1 and 2.

As seen in figures 1 and 2, for the majority of the satellite lines the corresponding contribution of cascades varies monotonically, mostly decreasing or remaining nearly constant for the various nuclear charges. An obvious exception is the q-satellite $1s^22s\,^2S_{1/2}$–$1s2p2s(^1P)\,^2P_{3/2}$, for which the correction function $\gamma(q, T_e)$ shows a prominent peak at $Z = 25$ (manganese) reaching a value of almost 1000. This satellite that is primarily populated via electron excitations from the ground state of the Li-like ion is often used for the determination of ionization balance and electron density [13, 14]. The strong peak in $\gamma(q, T_e)$ correlates with a similarly sharp drop in the autoionization probability A_a

Table 2. Autoionization rate A_a (in s^{-1}) for the K234 state and radiative transition probability A_r (in s^{-1}) and intensity factor Q_d for the q-satellite for several values of the nuclear charge Z.

Z	18	22	24	25	26	30
A_a	1.86×10^{12}	3.47×10^{11}	2.71×10^{10}	2.36×10^{9}	6.71×10^{10}	1.06×10^{12}
A_r	1.01×10^{14}	2.42×10^{14}	3.49×10^{14}	4.14×10^{14}	4.87×10^{14}	8.61×10^{14}
Q_d	7.32×10^{12}	1.39×10^{12}	1.08×10^{11}	9.46×10^{9}	2.68×10^{11}	4.25×10^{12}

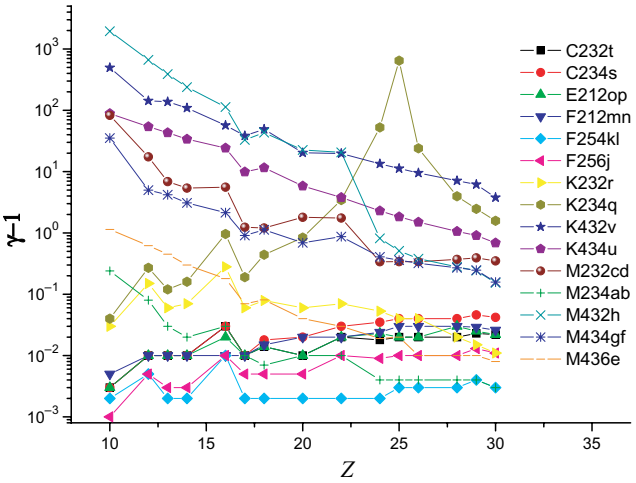

Figure 1. Deviation from the no-cascade case, $\gamma - 1$, as a function of Z for $T_e = 2 \times \mathrm{IP_{Li}}$.

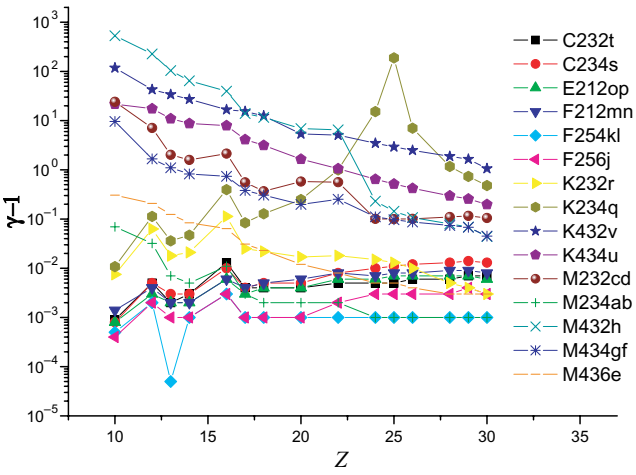

Figure 2. Deviation from the no-cascade case, $\gamma - 1$, as a function of Z for $T_e = 0.5 \times \mathrm{IP_{Li}}$.

for the upper level $1s2p2s(^1P)\,^2P_{3/2}$. Table 2 presents the corresponding A_a values for several elements from Ar to Zn as calculated using the MZ code. While the rates at $Z = 18$ and 30 are of the order of $10^{12}\ s^{-1}$, the autoionization probability for the $1s2p2s(^1P)\,^2P_{3/2}$ state in Li-like Mn drops to $2.36 \times 10^{9}\ s^{-1}$. Since the DC rate is directly proportional to the autoionization rate, this results in a very small DC probability as compared with the other population mechanisms for this level (cf figure 1(a) in [15]).

It seems that the calculated decrease in autoionization rate for the K234 state is due to an accidental cancellation in the corresponding matrix element. We studied the Z-dependence of the mixing coefficients in different coupling schemes and effects of configuration interaction, and in no case is there a noticeable change in the wavefunction behavior near

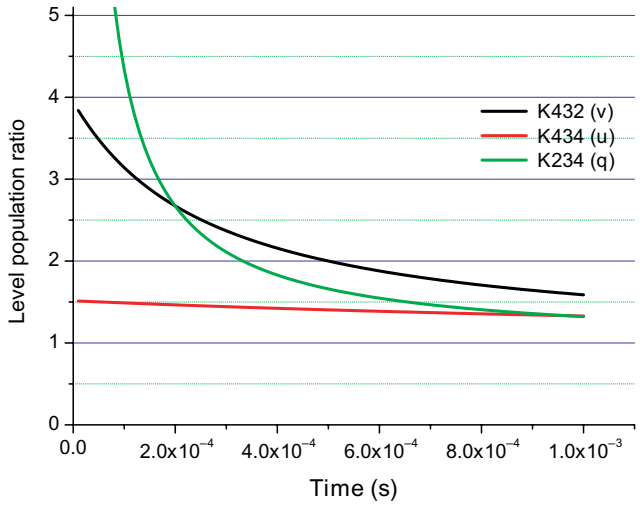

Figure 3. Ratios of upper level populations for three satellite lines with and without cascades for recombining Mn plasma.

$Z = 25$. Another state showing a sharp drop in the correction function is the M432 state, which is the upper level for the h- and i-satellites. Note also that M432 and K234 states have different J values, and thus there is no mixing between them. Besides, spin-forbidden transitions are extremely weak in all measured spectra to date.

In spite of the large correction factor for the q-satellite, for $Z = 25$ it turns out that for steady-state conditions the intensity of this line is still primarily affected by the inner-shell excitations from the ground state of the Li-like ion. This was confirmed by collisional–radiative simulations with the code NOMAD, which is described in detail elsewhere [16]. The required atomic parameters (energy levels, transition probabilities and collisional cross sections) for Li-, He- and H-like ions of Mn were calculated using the MZ and ATOM [8] codes. The Coulomb–Born-exchange method, implemented in ATOM for cross-section calculations, is applicable for such highly charged ions. Using NOMAD we calculated the line intensities of the $1s^2$–$1s2l$ transitions in Mn He-like ions and the corresponding satellites, for electron temperatures $T_e = 0.5 \times \mathrm{IP_{Li}}$, $\mathrm{IP_{Li}}$ and $2 \times \mathrm{IP_{Li}}$ ($\mathrm{IP_{Li}} = 940$ eV for Mn) and for the electron density of $N_e = 10^{14}\ cm^{-3}$. The intensities of the q and other satellites are modified by not more than a few per cent under steady-state conditions. The analysis of population channels shows that the inner-shell excitation flux that is proportional to the population of the $1s^22s$ ground state in the Li-like ion is dominant for all three temperatures.

Although the importance of cascades was found to be relatively low for steady-state conditions, the intensities of satellite lines with relatively low autoionization probabilities can be noticeably enhanced in transient plasmas due to

radiative cascades from high-n levels. For instance, when bare nuclei or H-like ions recombine in a relatively cold plasma, the density of the Li-like ion is negligibly small, and therefore the DC is the only significant channel to populate the doubly excited autoionizing states. In order to test this assumption, we performed simulation of the time-dependent recombination of Mn bare nuclei for electron temperature $T_e = 940$ eV and density $N_e = 10^{14}$ cm^{-3}. The system was allowed to evolve for 100 time steps, each of 10^{-5} s. Figure 3 presents the ratios of populations of the upper levels of the satellites q, u and v, calculated with and without radiative cascades. It is seen that at early times, the account of cascades indeed results in enhancements of these lines. As the system relaxes to a steady state, the difference between the two cases diminishes, as expected.

4. Conclusion

In conclusion, we presented a detailed calculation of radiative-cascade contributions to the intensities of dielectronic satellite lines of He_α (see the appendix). The correction function was calculated for elements with nuclear charges $Z = 10$–30. It was found that while for most of the satellites the cascade contribution varies smoothly and monotonically with Z, the q-satellite correction function has a sharp peak for Mn with its value reaching 1000. We also performed collisional–radiative calculations to confirm that (i) the low-density steady-state plasmas do not indicate significant enhancement of satellite intensities due to radiative cascades, and (ii) in a time-dependent recombining 10^{14} cm^{-3} plasma of Mn bare nuclei, the cascades can enhance the intensities of satellites such as q, u and v by a factor of 2–4. The derived results would be valid for a wide range of electron densities.

Acknowledgments

YuR thanks the members of the Plasma Laboratory of the Weizmann Institute of Science for their hospitality during the course of this work. This work was supported in part by the Israel Science Foundation and Minerva (Germany) Foundation.

Appendix. The correction function γ for autoionizing states $1s2l2l'$ as a function of the reduced electron temperature $t = T_e/IP_{Li}$.

	t											
	0.30	0.50	0.70	0.90	1.00	1.10	1.30	1.50	1.70	1.90	2.00	2.10
Neon ($Z = 10$)												
C 232	1.000	1.000	1.002	1.002	1.002	1.002	1.003	1.003	1.003	1.003	1.003	1.003
C 234	1.000	1.000	1.001	1.002	1.002	1.002	1.002	1.002	1.003	1.003	1.003	1.003
E 212	1.000	1.000	1.001	1.002	1.002	1.002	1.002	1.003	1.003	1.003	1.003	1.003
F 212	1.001	1.001	1.002	1.002	1.003	1.003	1.004	1.004	1.004	1.005	1.005	1.005
F 254	1.000	1.001	1.001	1.001	1.001	1.001	1.001	1.001	1.002	1.002	1.002	1.002
F 256	1.000	1.000	1.001	1.001	1.001	1.001	1.001	1.001	1.001	1.001	1.001	1.001
K 232	1.003	1.008	1.012	1.016	1.017	1.019	1.021	1.023	1.025	1.026	1.026	1.027
K 234	1.004	1.011	1.017	1.023	1.025	1.027	1.031	1.033	1.036	1.037	1.038	1.039
K 432	34.11	119.0	204.8	277.1	308.1	336.1	384.2	423.8	456.8	484.7	497.1	508.5
K 434	7.243	22.66	37.99	50.83	56.31	61.24	69.71	76.67	82.46	87.35	89.52	91.52
M 232	9.084	25.16	39.63	51.14	55.94	60.20	67.41	73.25	78.07	82.09	83.86	85.50
M 234	1.023	1.067	1.111	1.144	1.158	1.171	1.191	1.208	1.222	1.234	1.239	1.243
M 432	168.8	531.6	871.4	1147.	1263	1367.	1543.	1687.	1805.	1905.	1949.	1990.
M 434	4.041	10.62	16.76	21.75	23.84	25.71	28.89	31.48	33.62	35.42	36.21	36.95
M 436	1.096	1.306	1.505	1.666	1.734	1.795	1.899	1.984	2.054	2.113	2.139	2.163
Magnesium ($Z = 12$)												
C 232	1.002	1.005	1.007	1.008	1.009	1.009	1.010	1.010	1.011	1.0113	1.012	1.012
C 234	1.002	1.005	1.008	1.009	1.010	1.010	1.011	1.012	1.013	1.0130	1.013	1.013
E 212	1.001	1.003	1.005	1.00	1.006	1.007	1.007	1.008	1.008	1.0084	1.009	1.009
F 212	1.002	1.004	1.005	1.006	1.007	1.007	1.007	1.008	1.008	1.0086	1.009	1.009
F 254	1.001	1.002	1.003	1.003	1.004	1.004	1.004	1.004	1.004	1.0046	1.005	1.005
F 256	1.001	1.002	1.003	1.004	1.004	1.004	1.004	1.005	1.005	1.0049	1.005	1.005
K 232	1.029	1.063	1.088	1.106	1.113	1.119	1.130	1.138	1.145	1.1501	1.153	1.155
K 234	1.053	1.113	1.158	1.191	1.204	1.215	1.234	1.248	1.260	1.2700	1.274	1.278
K 432	15.95	43.81	68.55	88.14	96.28	103.5	115.7	125.6	133.8	140.58	143.6	146.4
K 434	7.575	18.49	27.80	35.04	38.02	40.65	45.09	48.66	51.59	54.035	55.11	56.10
M 232	4.278	8.095	10.95	13.03	13.86	14.58	15.77	16.72	17.49	18.116	18.39	18.65
M 234	1.015	1.032	1.044	1.053	1.056	1.059	1.065	1.069	1.072	1.0743	1.076	1.077
M 432	90.53	227.4	340.8	427.7	463.3	494.7	547.2	589.4	624.0	652.66	665.3	676.9
M 434	1.651	2.672	3.527	4.185	4.455	4.694	5.094	5.415	5.679	5.8977	5.994	6.083
M 436	1.081	1.208	1.314	1.395	1.428	1.457	1.506	1.545	1.578	1.6043	1.616	1.627
Aluminum ($Z = 13$)												
C 232	1.001	1.002	1.003	1.005	1.005	1.005	1.006	1.007	1.007	1.007	1.007	1.008
C 234	1.001	1.003	1.004	1.006	1.006	1.007	1.008	1.008	1.009	1.009	1.009	1.010
E 212	1.001	1.002	1.003	1.004	1.004	1.004	1.005	1.005	1.006	1.006	1.006	1.006
F 212	1.001	1.002	1.003	1.004	1.005	1.005	1.006	1.006	1.007	1.007	1.007	1.007
F 254	1.000	1.001	1.001	1.001	1.001	1.001	1.001	1.001	1.002	1.002	1.002	1.002
F 256	1.000	1.001	1.001	1.002	1.002	1.002	1.002	1.002	1.003	1.003	1.003	1.003
K 232	1.006	1.018	1.028	1.037	1.041	1.044	1.050	1.054	1.058	1.061	1.062	1.063
K 234	1.012	1.036	1.057	1.075	1.082	1.088	1.099	1.108	1.115	1.121	1.124	1.127

Appendix. Continued

	t											
	0.30	0.50	0.70	0.90	1.00	1.10	1.30	1.50	1.70	1.90	2.00	2.10
K 432	10.85	34.95	58.83	78.79	87.30	94.95	108.1	118.9	127.8	135.4	138.8	141.9
K 434	4.271	11.95	19.43	25.63	28.26	30.62	34.66	37.97	40.73	43.04	44.07	45.02
M 232	1.684	3.021	4.221	5.173	5.570	5.922	6.518	7.001	7.398	7.731	7.877	8.012
M 234	1.002	1.007	1.012	1.015	1.017	1.018	1.020	1.022	1.024	1.025	1.026	1.026
M 432	33.40	105.1	172.9	228.2	251.5	272.4	308.0	337.0	361.0	381.2	390.1	398.4
M 434	1.338	2.102	2.832	3.431	3.683	3.910	4.296	4.612	4.874	5.094	5.191	5.281
M 436	1.040	1.124	1.202	1.266	1.293	1.316	1.357	1.390	1.417	1.440	1.450	1.460
Silicon ($Z = 14$)												
C 232	1.001	1.003	1.004	1.006	1.006	1.007	1.007	1.008	1.009	1.009	1.009	1.009
C 234	1.001	1.003	1.005	1.007	1.007	1.008	1.009	1.010	1.010	1.011	1.011	1.011
E 212	1.001	1.002	1.003	1.004	1.005	1.005	1.006	1.006	1.007	1.007	1.007	1.008
F 212	1.001	1.002	1.004	1.005	1.005	1.006	1.006	1.007	1.007	1.008	1.008	1.008
F 254	1.000	1.001	1.001	1.001	1.001	1.001	1.001	1.001	1.002	1.002	1.002	1.002
F 256	1.000	1.001	1.001	1.002	1.002	1.002	1.003	1.003	1.003	1.003	1.003	1.003
K 232	1.007	1.021	1.034	1.044	1.048	1.052	1.058	1.064	1.068	1.071	1.073	1.075
K 234	1.016	1.047	1.075	1.097	1.107	1.115	1.129	1.140	1.150	1.158	1.161	1.164
K 432	8.968	28.20	47.14	62.91	69.62	75.66	86.00	94.49	101.6	107.5	110.1	112.6
K 434	3.648	9.744	15.63	20.48	22.53	24.37	27.52	30.10	32.24	34.04	34.84	35.58
M 232	1.539	2.589	3.528	4.273	4.582	4.858	5.323	5.700	6.010	6.270	6.384	6.489
M 234	1.002	1.005	1.009	1.011	1.012	1.013	1.015	1.016	1.017	1.018	1.018	1.019
M 432	21.26	65.47	107.0	140.9	155.1	167.8	189.5	207.2	221.8	234.1	239.5	244.5
M 434	1.256	1.824	2.363	2.803	2.989	3.155	3.438	3.669	3.860	4.021	4.092	4.158
M 436	1.027	1.084	1.137	1.180	1.198	1.214	1.241	1.263	1.282	1.297	1.304	1.310
Sulfur ($Z = 16$)												
C 232	1.006	1.013	1.018	1.022	1.023	1.024	1.027	1.028	1.030	1.031	1.031	1.032
C 234	1.005	1.010	1.014	1.017	1.019	1.020	1.022	1.023	1.024	1.025	1.026	1.026
E 212	1.003	1.006	1.009	1.012	1.013	1.014	1.015	1.016	1.017	1.018	1.018	1.018
F 212	1.002	1.006	1.008	1.010	1.011	1.011	1.012	1.013	1.014	1.015	1.015	1.015
F 254	1.001	1.003	1.004	1.005	1.006	1.006	1.006	1.007	1.007	1.007	1.008	1.008
F 256	1.001	1.003	1.005	1.006	1.006	1.006	1.007	1.008	1.008	1.008	1.008	1.009
K 232	1.051	1.113	1.160	1.195	1.208	1.220	1.240	1.256	1.268	1.279	1.284	1.288
K 234	1.182	1.396	1.554	1.669	1.714	1.754	1.819	1.871	1.913	1.947	1.962	1.976
K 432	6.745	17.70	27.56	35.44	38.72	41.64	46.60	50.61	53.93	56.70	57.92	59.05
K 434	4.019	8.921	13.08	16.30	17.63	18.81	20.78	22.37	23.67	24.76	25.24	25.68
M 232	1.939	3.140	4.071	4.761	5.039	5.282	5.686	6.008	6.269	6.485	6.580	6.667
M 234	1.005	1.011	1.015	1.018	1.019	1.020	1.022	1.023	1.025	1.026	1.026	1.026
M 432	17.21	40.73	59.91	74.49	80.44	85.68	94.45	101.5	107.2	112.0	114.1	116.0
M 434	1.298	1.739	2.102	2.380	2.494	2.594	2.762	2.896	3.006	3.098	3.138	3.175
M 436	1.026	1.064	1.095	1.119	1.129	1.137	1.152	1.163	1.173	1.180	1.184	1.187
Chlorine ($Z = 17$)												
C 232	1.001	1.004	1.007	1.008	1.009	1.010	1.011	1.012	1.013	1.014	1.014	1.014
C 234	1.001	1.004	1.006	1.008	1.009	1.010	1.011	1.012	1.013	1.014	1.014	1.014
E 212	1.001	1.003	1.005	1.007	1.008	1.008	1.010	1.010	1.011	1.012	1.012	1.012
F 212	1.001	1.004	1.006	1.008	1.008	1.009	1.010	1.011	1.012	1.012	1.012	1.013
F 254	1.000	1.001	1.001	1.001	1.001	1.001	1.001	1.002	1.002	1.002	1.002	1.002
F 256	1.000	1.001	1.002	1.003	1.003	1.003	1.004	1.004	1.004	1.004	1.005	1.005
K 232	1.008	1.025	1.040	1.052	1.057	1.062	1.070	1.076	1.081	1.085	1.087	1.089
K 234	1.028	1.084	1.134	1.175	1.192	1.206	1.232	1.252	1.269	1.284	1.290	1.296
K 432	5.571	16.39	26.96	35.72	39.44	42.79	48.51	53.20	57.10	60.39	61.84	63.19
K 434	2.296	5.128	7.798	9.976	10.89	11.72	13.11	14.25	15.20	15.99	16.34	16.67
M 232	1.192	1.557	1.881	2.136	2.242	2.336	2.495	2.623	2.729	2.817	2.856	2.892
M 234	1.001	1.003	1.004	1.005	1.006	1.006	1.007	1.008	1.008	1.008	1.009	1.009
M 432	5.486	14.98	23.80	30.94	33.93	36.61	41.16	44.86	47.93	50.50	51.63	52.68
M 434	1.120	1.381	1.624	1.823	1.906	1.981	2.107	2.211	2.296	2.368	2.400	2.429
M 436	1.010	1.031	1.050	1.065	1.072	1.078	1.087	1.095	1.102	1.107	1.110	1.112
Argon ($Z = 18$)												
C 232	1.001	1.004	1.006	1.008	1.009	1.010	1.011	1.012	1.013	1.014	1.014	1.014
C 234	1.002	1.005	1.008	1.011	1.012	1.012	1.014	1.015	1.016	1.017	1.018	1.018
E 212	1.001	1.004	1.006	1.008	1.009	1.010	1.011	1.012	1.013	1.013	1.014	1.014
F 212	1.002	1.005	1.007	1.009	1.010	1.011	1.012	1.013	1.014	1.015	1.015	1.015
F 254	1.000	1.001	1.001	1.001	1.001	1.001	1.001	1.002	1.002	1.002	1.002	1.002
F 256	1.000	1.001	1.002	1.003	1.003	1.004	1.004	1.004	1.005	1.005	1.005	1.005
K 232	1.007	1.022	1.036	1.047	1.052	1.056	1.063	1.069	1.073	1.077	1.079	1.081
K 234	1.043	1.128	1.205	1.266	1.292	1.315	1.353	1.385	1.410	1.432	1.441	1.450
K 432	4.711	13.46	21.98	29.05	32.05	34.74	39.35	43.13	46.27	48.91	50.08	51.17

Appendix. Continued

	t											
	0.30	0.50	0.70	0.90	1.00	1.10	1.30	1.50	1.70	1.90	2.00	2.10
K 434	1.997	4.147	6.162	7.800	8.490	9.106	10.16	11.01	11.72	12.31	12.57	12.82
M 232	1.129	1.367	1.577	1.741	1.810	1.870	1.972	2.055	2.122	2.179	2.204	2.227
M 234	1.001	1.002	1.003	1.004	1.005	1.005	1.006	1.006	1.007	1.007	1.007	1.007
M 432	4.657	2.629	20.15	26.27	28.86	31.17	35.10	38.31	40.97	43.21	44.19	45.10
M 434	1.097	1.306	1.503	1.662	1.729	1.789	1.891	1.974	2.043	2.101	2.126	2.150
M 436	1.008	1.023	1.037	1.049	1.053	1.058	1.065	1.071	1.075	1.079	1.081	1.083
Calcium ($Z = 20$)												
C 232	1.001	1.004	1.006	1.008	1.009	1.009	1.010	1.011	1.012	1.013	1.013	1.013
C 234	1.002	1.005	1.008	1.011	1.012	1.013	1.014	1.016	1.017	1.017	1.018	1.018
E 212	1.001	1.004	1.006	1.008	1.009	1.010	1.011	1.012	1.013	1.013	1.014	1.014
F 212	1.002	1.006	1.009	1.012	1.013	1.014	1.015	1.017	1.018	1.019	1.019	1.019
F 254	1.000	1.001	1.001	1.002	1.002	1.002	1.002	1.002	1.002	1.003	1.003	1.003
F 256	1.000	1.001	1.002	1.003	1.003	1.003	1.004	1.004	1.004	1.005	1.005	1.005
K 232	1.006	1.017	1.028	1.036	1.039	1.043	1.048	1.052	1.055	1.058	1.060	1.061
K 234	1.085	1.249	1.396	1.512	1.561	1.604	1.676	1.735	1.784	1.824	1.842	1.859
K 432	2.660	6.371	9.904	12.80	14.02	15.12	16.98	18.51	19.77	20.84	21.31	21.74
K 434	1.539	2.647	3.664	4.481	4.823	5.128	5.646	6.066	6.413	6.704	6.833	6.951
M 232	1.212	1.578	1.890	2.131	2.230	2.317	2.464	2.583	2.679	2.760	2.795	2.828
M 234	1.001	1.002	1.003	1.003	1.004	1.004	1.004	1.005	1.005	1.005	1.005	1.006
M 432	3.420	7.892	11.81	14.89	16.17	17.30	19.20	20.74	22.01	23.06	23.53	23.96
M 434	1.066	1.198	1.317	1.413	1.453	1.488	1.548	1.597	1.637	1.671	1.686	1.699
M 436	1.004	1.012	1.018	1.024	1.026	1.028	1.032	1.034	1.037	1.039	1.039	1.040
Titanium ($Z = 22$)												
C 232	1.002	1.005	1.008	1.010	1.011	1.012	1.013	1.014	1.015	1.016	1.016	1.017
C 234	1.003	1.008	1.013	1.017	1.018	1.020	1.022	1.024	1.026	1.027	1.028	1.028
E 212	1.002	1.006	1.009	1.012	1.013	1.014	1.016	1.017	1.019	1.020	1.020	1.021
F 212	1.003	1.008	1.012	1.015	1.017	1.018	1.020	1.022	1.023	1.024	1.025	1.025
F 254	1.000	1.001	1.001	1.001	1.001	1.001	1.002	1.002	1.002	1.002	1.002	1.002
F 256	1.001	1.002	1.003	1.004	1.005	1.005	1.006	1.006	1.007	1.007	1.007	1.007
K 232	1.00	1.018	1.030	1.039	1.043	1.046	1.052	1.057	1.061	1.064	1.065	1.067
K 234	1.334	1.996	2.595	3.074	3.274	3.452	3.753	3.998	4.200	4.368	4.443	4.512
K 432	2.529	6.070	9.495	12.32	13.52	14.60	16.44	17.94	19.19	20.241	20.71	21.14
K 434	1.344	2.059	2.720	3.252	3.475	3.674	4.013	4.288	4.515	4.706	4.790	4.868
M 232	1.206	1.562	1.866	2.100	2.197	2.282	2.425	2.540	2.634	2.713	2.747	2.779
M 234	1.001	1.002	1.002	1.003	1.003	1.004	1.004	1.005	1.005	1.005	1.005	1.005
M 432	3.333	7.499	11.09	13.88	15.03	16.05	17.76	19.14	20.27	21.21	21.63	22.01
M 434	1.085	1.252	1.403	1.523	1.574	1.618	1.694	1.755	1.806	1.848	1.867	1.884
M 436	1.003	1.008	1.013	1.017	1.019	1.021	1.023	1.025	1.027	1.028	1.029	1.029
Chromium ($Z = 24$)												
C 232	1.002	1.005	1.008	1.011	1.012	1.013	1.014	1.015	1.016	1.017	1.018	1.018
C 234	1.003	1.010	1.016	1.021	1.023	1.025	1.028	1.030	1.032	1.034	1.035	1.035
E 212	1.002	1.006	1.010	1.014	1.015	1.016	1.018	1.020	1.021	1.022	1.023	1.023
F 212	1.003	1.007	1.012	1.015	1.016	1.018	1.020	1.021	1.023	1.024	1.024	1.025
F 254	1.000	1.001	1.001	1.001	1.002	1.002	1.002	1.002	1.002	1.002	1.002	1.002
F 256	1.001	1.003	1.004	1.005	1.006	1.006	1.007	1.008	1.008	1.009	1.009	1.009
K 232	1.005	1.015	1.024	1.031	1.035	1.037	1.042	1.046	1.049	1.052	1.053	1.054
K 234	6.125	16.24	25.39	32.68	35.72	38.49	43.01	46.73	49.80	52.37	53.50	54.54
K 432	2.054	4.471	6.799	8.716	9.528	10.26	11.50	12.52	13.36	14.08	14.39	14.68
K 434	1.210	1.644	2.043	2.365	2.500	2.620	2.824	2.990	3.127	3.242	3.293	3.340
M 232	1.035	1.101	1.160	1.207	1.227	1.244	1.273	1.296	1.316	1.332	1.339	1.346
M 234	1.000	1.001	1.002	1.002	1.003	1.003	1.003	1.004	1.004	1.004	1.004	1.004
M 432	1.076	1.231	1.373	1.487	1.535	1.578	1.650	1.709	1.757	1.798	1.816	1.832
M 434	1.035	1.111	1.182	1.240	1.264	1.286	1.322	1.352	1.377	1.398	1.407	1.415
M 436	1.002	1.005	1.009	1.011	1.012	1.013	1.015	1.016	1.017	1.018	1.019	1.019
Manganese ($Z = 25$)												
C 232	1.002	1.005	1.009	1.011	1.012	1.013	1.015	1.016	1.017	1.018	1.018	1.019
C 234	1.004	1.011	1.017	1.023	1.025	1.027	1.030	1.033	1.035	1.037	1.038	1.038
E 212	1.002	1.007	1.011	1.014	1.016	1.017	1.019	1.021	1.022	1.024	1.024	1.025
F 212	1.003	1.008	1.012	1.016	1.017	1.018	1.020	1.022	1.024	1.025	1.025	1.026
F 254	1.000	1.001	1.001	1.002	1.002	1.002	1.002	1.002	1.002	1.002	1.003	1.003
F 256	1.001	1.003	1.004	1.006	1.006	1.007	1.008	1.008	1.009	1.009	1.009	1.010
K 232	1.004	1.013	1.020	1.027	1.029	1.032	1.036	1.039	1.041	1.044	1.045	1.046
K 234	64.48	189.3	301.8	391.4	428.8	462.1	518.4	564.1	601.7	633.2	647.1	659.9
K 432	1.892	3.925	5.878	7.484	8.165	8.774	9.816	10.67	11.37	11.97	12.23	12.48

Appendix. Continued

	t											
	0.30	0.50	0.70	0.90	1.00	1.10	1.30	1.50	1.70	1.90	2.00	2.10
K 434	1.168	1.516	1.835	2.092	2.200	2.296	2.459	2.592	2.701	2.793	2.834	2.871
M 232	1.035	1.100	1.159	1.205	1.224	1.241	1.270	1.293	1.313	1.329	1.336	1.342
M 234	1.000	1.001	1.002	1.002	1.003	1.003	1.003	1.003	1.004	1.004	1.004	1.004
M 432	1.047	1.144	1.234	1.306	1.336	1.363	1.408	1.446	1.476	1.502	1.513	1.524
M 434	1.031	1.097	1.159	1.209	1.230	1.249	1.281	1.308	1.329	1.347	1.356	1.363
M 436	1.002	1.005	1.007	1.009	1.010	1.011	1.013	1.014	1.015	1.015	1.016	1.016
Iron ($Z = 26$)												
C 232	1.002	1.006	1.009	1.012	1.013	1.014	1.015	1.017	1.018	1.019	1.019	1.019
C 234	1.004	1.012	1.019	1.024	1.027	1.029	1.032	1.035	1.037	1.039	1.040	1.041
E 212	1.002	1.007	1.011	1.015	1.016	1.017	1.020	1.022	1.023	1.024	1.025	1.025
F 212	1.003	1.008	1.013	1.016	1.018	1.019	1.021	1.023	1.025	1.026	1.026	1.027
F 254	1.000	1.001	1.001	1.002	1.002	1.002	1.002	1.002	1.003	1.003	1.003	1.003
F 256	1.001	1.003	1.005	1.006	1.007	1.007	1.008	1.009	1.009	1.010	1.010	1.010
K 232	1.003	1.010	1.016	1.021	1.023	1.025	1.028	1.031	1.033	1.034	1.035	1.036
K 234	3.380	8.029	12.21	15.53	16.92	18.15	20.24	21.93	23.32	24.49	25.00	25.48
K 432	1.764	3.493	5.148	6.508	7.084	7.600	8.480	9.200	9.797	10.300	10.522	10.727
K 434	1.138	1.421	1.682	1.893	1.981	2.059	2.192	2.301	2.390	2.465	2.498	2.529
M 232	1.035	1.101	1.160	1.207	1.227	1.244	1.273	1.297	1.316	1.333	1.340	1.347
M 234	1.000	1.001	1.002	1.002	1.003	1.003	1.003	1.003	1.004	1.004	1.004	1.004
M 432	1.035	1.107	1.174	1.227	1.250	1.270	1.304	1.331	1.354	1.373	1.382	1.389
M 434	1.028	1.087	1.143	1.188	1.207	1.224	1.253	1.276	1.295	1.312	1.319	1.326
M 436	1.001	1.004	1.006	1.008	1.009	1.010	1.011	1.012	1.012	1.013	1.013	1.014
Nickel ($Z = 28$)												
C 232	1.002	1.006	1.010	1.013	1.014	1.015	1.017	1.019	1.020	1.021	1.021	1.022
C 234	1.004	1.013	1.021	1.027	1.029	1.032	1.036	1.039	1.041	1.043	1.044	1.045
E 212	1.002	1.007	1.011	1.015	1.016	1.018	1.020	1.022	1.023	1.025	1.025	1.026
F 212	1.003	1.009	1.014	1.017	1.019	1.020	1.023	1.025	1.026	1.028	1.028	1.029
F 254	1.000	1.001	1.002	1.002	1.002	1.002	1.003	1.003	1.003	1.003	1.003	1.003
F 256	1.001	1.003	1.006	1.007	1.008	1.008	1.010	1.010	1.011	1.012	1.012	1.012
K 232	1.002	1.005	1.008	1.011	1.012	1.013	1.014	1.016	1.017	1.018	1.018	1.018
K 234	1.401	2.173	2.863	3.409	3.637	3.839	4.181	4.457	4.685	4.876	4.960	5.037
K 432	1.583	2.880	4.115	5.126	5.553	5.935	6.587	7.120	7.562	7.933	8.097	8.249
K 434	1.097	1.297	1.481	1.629	1.691	1.746	1.840	1.916	1.979	2.032	2.055	2.077
M 232	1.038	1.110	1.174	1.226	1.247	1.266	1.298	1.324	1.345	1.363	1.371	1.378
M 234	1.000	1.001	1.002	1.002	1.003	1.003	1.003	1.003	1.004	1.004	1.004	1.004
M 432	1.026	1.080	1.129	1.169	1.186	1.200	1.225	1.246	1.263	1.277	1.283	1.289
M 434	1.024	1.074	1.121	1.159	1.175	1.189	1.214	1.234	1.250	1.264	1.270	1.275
M 436	1.001	1.003	1.005	1.007	1.007	1.008	1.009	1.009	1.010	1.011	1.011	1.011
Copper ($Z = 29$)												
C 232	1.002	1.007	1.011	1.014	1.015	1.017	1.019	1.020	1.021	1.023	1.023	1.023
C 234	1.005	1.014	1.022	1.028	1.031	1.033	1.037	1.040	1.043	1.045	1.046	1.047
E 212	1.002	1.007	1.011	1.015	1.016	1.018	1.020	1.022	1.023	1.025	1.025	1.026
F 212	1.003	1.009	1.014	1.018	1.019	1.021	1.023	1.025	1.027	1.028	1.029	1.029
F 254	1.000	1.001	1.002	1.002	1.002	1.003	1.003	1.003	1.003	1.003	1.004	1.004
F 256	1.001	1.004	1.006	1.008	1.008	1.009	1.010	1.011	1.012	1.012	1.013	1.013
K 232	1.001	1.004	1.007	1.009	1.010	1.010	1.012	1.013	1.014	1.014	1.015	1.015
K 234	1.252	1.735	2.165	2.505	2.646	2.772	2.984	3.156	3.298	3.416	3.468	3.516
K 432	1.515	2.648	3.723	4.601	4.972	5.303	5.869	6.331	6.714	7.035	7.178	7.309
K 434	1.084	1.256	1.414	1.542	1.595	1.643	1.724	1.790	1.844	1.889	1.909	1.928
M 232	1.040	1.116	1.184	1.238	1.261	1.281	1.315	1.342	1.365	1.384	1.392	1.400
M 234	1.000	1.001	1.002	1.002	1.003	1.003	1.003	1.003	1.004	1.004	1.004	1.004
M 432	1.022	1.069	1.111	1.145	1.160	1.172	1.194	1.211	1.226	1.238	1.243	1.248
M 434	1.022	1.068	1.111	1.146	1.160	1.174	1.196	1.214	1.229	1.242	1.247	1.252
M 436	1.001	1.003	1.005	1.006	1.007	1.007	1.008	1.009	1.009	1.010	1.010	1.010
Zinc ($Z = 30$)												
C 232	1.002	1.007	1.011	1.014	1.015	1.016	1.018	1.019	1.021	1.022	1.022	1.022
C 234	1.004	1.013	1.020	1.026	1.028	1.030	1.034	1.037	1.039	1.041	1.042	1.043
E 212	1.002	1.006	1.010	1.013	1.015	1.016	1.018	1.019	1.021	1.022	1.022	1.023
F 212	1.003	1.008	1.012	1.016	1.017	1.019	1.021	1.023	1.024	1.025	1.026	1.026
F 254	1.000	1.001	1.002	1.002	1.002	1.002	1.003	1.003	1.003	1.003	1.003	1.003
F 256	1.001	1.003	1.005	1.007	1.007	1.008	1.009	1.010	1.010	1.011	1.011	1.011
K 232	1.001	1.003	1.005	1.007	1.008	1.008	1.009	1.010	1.011	1.011	1.011	1.012
K 234	1.167	1.479	1.754	1.970	2.060	2.140	2.274	2.382	2.471	2.546	2.579	2.609

Appendix. Continued

	t											
	0.30	0.50	0.70	0.90	1.00	1.10	1.30	1.50	1.70	1.90	2.00	2.10
K 432	1.346	2.061	2.719	3.250	3.473	3.671	4.008	4.282	4.509	4.699	4.782	4.860
K 434	1.066	1.198	1.318	1.414	1.454	1.489	1.550	1.599	1.639	1.673	1.688	1.701
M 232	1.037	1.105	1.166	1.214	1.234	1.252	1.282	1.306	1.326	1.343	1.350	1.357
M 234	1.000	1.001	1.002	1.002	1.002	1.002	1.003	1.003	1.003	1.003	1.003	1.003
M 432	1.015	1.044	1.071	1.092	1.101	1.109	1.123	1.133	1.142	1.150	1.153	1.156
M 434	1.015	1.045	1.072	1.095	1.104	1.112	1.126	1.138	1.147	1.155	1.158	1.162
M 436	1.001	1.003	1.004	1.005	1.006	1.006	1.007	1.007	1.008	1.008	1.008	1.009

References

[1] Dubau J and Volonte S 1980 *Rep. Prog. Phys.* **43** 199

[2] Presnyakov L P 1976 *Usp. Fiz. Nauk* **119** 49 (in Russian)

[3] Eric H Silver and Steven M Kahn (eds) 1993 *UV and X-Ray Spectroscopy of Laboratory and Astrophysical Plasmas* (Cambridge: Cambridge University Press)

[4] Karim K R and Bhala C P 1988 *Phys. Rev.* A **37** 840

[5] Marchuk O, Bertschinger G, Kunze H-J, Badnell N R and Fritzsche S 2004 *J. Phys. B: At. Mol. Opt. Phys.* **37** 1951

[6] Steenman-Clark L, Bely-Dubau F and Faucher P 1980 *Mon. Not. R. Astron. Soc.* **191** 951

[7] Gabriel A H 1972 *Mon. Not. R. Astron. Soc.* **160** 99

[8] Shevelko V P and Vainshtein L A 1993 *Atomic Physics for Hot Plasmas* (Bristol: IPP)

[9] Goryayev F F, Urnov A M and Vainshtein L A 2006 *Atomic data calculations by Z-expansion method for doubly excited states $2lnl'$ and $1s2lnl'$ of highly charged ions with $Z = 6$–36. I. Transitions from the states with $n = 2, 3$.* arXiv:physics/0603164 v2 3 Apr 2006 http://arxiv.org/abs/physics/0603164

[10] Vainshtein L A and Safronova U I 1978 *At. Data Nucl. Data Tables* **21** 49

[11] Yamamoto N, Kato T and Rosmej F B 2005 *J. Quant. Spectrosc. Radiat. Transfer* **96** 343

[12] Wang J G, Kato T and Murakami I 1999 *Phys. Rev.* **60** 2104

[13] Lunney J G 1983 *J. Phys. B: At. Mol. Phys.* **16** L83–7

[14] Mancini R C, Audebert P, Geindre J P, Rousse A, Fallies F, Gauthier J C, Mysyrowicz A, Chambaret J P and Antonetti A 1994 *J. Phys. B: At. Mol. Opt. Phys.* **27** 1671–81

[15] Safronova U I, Safronova M S and Bruch R 1995 *J. Phys. B: At. Mol. Opt. Phys.* **28** 2803–16

[16] Ralchenko Yu V and Maron Y 2001 *J. Quant. Spectrosc. Radiat. Transfer* **71** 609